Journal of Thermal Analysis and Calorimetry, Vol. 95 (2009) 2, 397–402

HEAT CAPACITY, ENTHALPY AND ENTROPY OF CALCIUM NIOBATES

J. Leitner[1*], *K. Růžička*[2], *D. Sedmidubský*[3] *and P. Svoboda*[4]

[1]Department of Solid State Engineering, Institute of Chemical Technology Prague, Technická 5, 166 28 Prague 6, Czech Republic
[2]Department of Physical Chemistry, Institute of Chemical Technology Prague, Technická 5, 166 28 Prague 6, Czech Republic
[3]Department of Inorganic Chemistry, Institute of Chemical Technology Prague, Technická 5, 166 28 Prague 6, Czech Republic
[4]Department of Condensed Matter Physics, Faculty of Mathematics and Physics, Charles University, Ke Karlovu 5, 120 00 Prague 2 Czech Republic

Heat capacity and enthalpy increments of calcium niobates $CaNb_2O_6$ and $Ca_2Nb_2O_7$ were measured by the relaxation time method (2–300 K), DSC (260–360 K) and drop calorimetry (669–1421 K). Temperature dependencies of the molar heat capacity in the form $C_{pm}=200.4+0.03432T-3.450\cdot10^6/T^2$ J K^{-1} mol^{-1} for $CaNb_2O_6$ and $C_{pm}=257.2+0.03621T-4.435\cdot10^6/T^2$ J K^{-1} mol^{-1} for $Ca_2Nb_2O_7$ were derived by the least-squares method from the experimental data. The molar entropies at 298.15 K, S^0_m($CaNb_2O_6$, 298.15 K)=167.3±0.9 J K^{-1} mol^{-1} and S^0_m($Ca_2Nb_2O_7$, 298.15 K)=212.4±1.2 J K^{-1} mol^{-1}, were evaluated from the low temperature heat capacity measurements. Standard enthalpies of formation at 298.15 K were derived using published values of Gibbs energy of formation and presented heat capacity and entropy data: Δ_fH^0($CaNb_2O_6$, 298.15 K)= –2664.52 kJ mol^{-1} and Δ_fH^0($Ca_2Nb_2O_7$, 298.15 K)= –3346.91 kJ mol^{-1}.

Keywords: *calcium niobates, drop calorimetry, DSC, enthalpy increments, enthalpy of formation, entropy, heat capacity, oxides*

Introduction

Phase equilibria in the CaO–Nb_2O_5 system have been studied by three different groups [1–3] and four equilibrium interoxide phases have been detected: calcium metaniobate $CaNb_2O_6$ (CN) with columbite-type structure, calcium pyroniobate $Ca_2Nb_2O_7$ (C2N) with monoclinic perovskite- slab-type structure, '$Ca_3Nb_2O_8$' (C3N) phase with nominal composition CaO:Nb_2O_5=75.25:24.75 and various polymorphs of a non-stoichiometric '$Ca_4Nb_2O_9$' (C4N) with perovskite-related structure. Although calcium niobates are considered as advanced materials showing some interesting electrical and optical properties as well as photocatalytic activity, only very limited information on thermodynamic properties of these mixed oxides are available now.

Dneprova *et al.* [4] have measured electromotive force (EMF) of galvanic cells with CaF_2 solid electrolyte. They derived Gibbs energies and enthalpies of formation of calcium niobates CN and C2N from the elements at temperatures 1000–1400 K. The results were recalculated [5] and, in the case of CN, were accepted in the reference tables [6]: Δ_fH^0(CN, 298.15 K)= –2675.249 J mol^{-1} and S^0_m(CN, 298.15 K)=178.448 J K^{-1} mol^{-1}. The temperature dependence of molar heat capacity of CN was estimated in [6]. On the basis of EMF measurements of galvanic cells with CaF_2 solid electrolyte, Raghavan [7, 8] has derived the Gibbs energy of formation of CN and C2N from the constituent binary oxides (CaO+Nb_2O_5) at temperatures 1225–1300 K. No experimental data on heat capacity of CN and/or C2N have been published yet.

In a systematic study of thermochemical properties of complex oxides in the Bi_2O_3–CaO–SrO–Nb_2O_5–Ta_2O_5 system, we have recently measured heat capacities and enthalpy increments of $Bi_2Ca_2O_5$, Bi_2CaO_4, $Bi_6Ca_4O_{13}$, $Bi_{14}Ca_5O_{26}$ [9], $BiNbO_4$, $BiTaO_4$ [10], $BiNb_5O_{14}$ [11], $SrBi_2Nb_2O_9$, $SrBi_2Ta_2O_9$ [12] and $SrNb_2O_6$ [13]. The goal of the present work is the measurement of heat capacity and enthalpy increments of calcium niobates CN and C2N in a broad temperature range, and evaluation of the standard molar entropy of these ternary oxides at 298.15 K, as well as the temperature dependence of C_{pm} above room temperature. Further, the standard enthalpies of formation of CN and C2N at 298.15 K were derived from Raghavan's EMF measurements.

Experimental

The samples were prepared by conventional solid-state reactions from high purity precursors $CaCO_3$ (99.9%, Aldrich) and Nb_2O_5 (99.85%, Alfa Aesar). The stoichiometric amounts of $CaCO_3$ and Nb_2O_5

---

[*] Author for correspondence: Jindrich.Leitner@vscht.cz

1388–6150/$20.00

Akadémiai Kiadó, Budapest, Hungary
Springer, Dordrecht, The Netherlands

were ground in agate mortar and calcinated at 1073 K in a platinum crucible in air atmosphere for 48 h. After regrinding, the mixtures were fired at 1173 K in air for 142 h. As the 1:1 sample did not contain only desired compound CN it was fired once more at 1223 K for 162 h.

X-ray powder diffraction data were collected at room temperature with an X'Pert PRO (PANalytical, the Netherlands) θ–θ powder diffractometer with parafocusing Bragg–Brentano geometry using CuK$_\alpha$ radiation (λ=1.5418 Å, U=40 kV, I=30 mA). The data were scanned over the angular range 5–60° (2θ) with an increment of 0.02° (2θ) and a counting time of 0.3 s step^{-1}. Data evaluation was performed by means of the HighScore Plus software package.

The PPMS equipment 14 T-type (Quantum Design, USA) was used for the heat capacity measurements in the low-temperature region. The measurements were performed by the relaxation method [14] with fully automatic procedure under high vacuum (pressure ~10^{-2} Pa) to avoid heat loss through the exchange gas. The samples were compressed powder plates of about 15 mg. The densities of the pressed samples were about 65% of the theoretical ones. The samples were mounted to the calorimeter platform with cryogenic grease Apiezon N (supplied by Quantum Design). The procedure was as follows: First, a blank sample holder with the Apiezon only was measured in the temperature range 2–300 K to obtain background data, then the sample plate was attached to the calorimeter platform and the measurement was repeated in the same temperature range with the same temperature steps. The sample heat capacity was then obtained as a difference between the two data sets. This procedure was applied, because the heat capacity of Apiezon is not negligible in comparison with the heat capacity of the sample (~8% at room temperature) and exhibits a sol–gel transition below room temperature [15]. The manufacturer claims the precision of this measurement better than 2% [16]; the control measurement of the copper sample (99.999% purity) confirmed this precision at least below 250 K. However, the precision of the measurement strongly depends on the thermal coupling between the sample and the calorimeter platform. Due to unavoidable porosity of the sample plate this coupling rapidly worsens at temperatures above 270 K as Apiezon diffuses into the porous sample and the uncertainty tends to be larger.

A Micro DSC III calorimeter (Setaram, France) in the incremental temperature scanning mode with a number of 5–10 K steps (heating rate 0.2 K min^{-1}) followed by isothermal delays of 9000 s was used for the heat capacity determination in the temperature range of 260–360 K. Synthetic sapphire, NIST Standard reference material No. 720, was used as the reference material. The typical sample mass was 0.7–0.9 g. The uncertainty of heat capacity measurements is estimated to be better than ±1%.

Enthalpy increment determinations were carried out by drop method using high temperature calorimeter, Multi HTC 96 (Setaram, France). All measurements were performed in air by alternating dropping of the reference material (small pieces of synthetic sapphire, NIST Standard reference material No. 720) and of the sample (CN or C2N pellets, 5 mm in diameter, thickness of 1–2 mm) being initially held at room temperature (T_0), through a lock into the working cell of the preheated calorimeter. Endothermic effects are detected and the relevant peak area is proportional to the heat content of the dropped specimen. The measurements were performed at temperatures 669–1421 K on samples of 105–175 mg. The delays between two subsequent drops were 40–50 min. To check the accuracy of measurement, the heat content of platinum at 500, 700, 900 and 1100°C was measured first and compared with reference values [17]. The standard deviation of 17 runs is 0.48 kJ mol^{-1}, average relative error 2.0%. Estimated overall accuracy of the drop measurements is ±3 %.

Results and discussion

The XRD analysis revealed that the prepared samples were without any observable diffraction lines from unreacted precursors or other phases. The CN sample was orthorhombic (space group Pbcn). The following lattice parameters were evaluated by Rietveld refinement: a=1.496976±0.000052 nm, b=0.574724±0.000020 nm, c=0.522022±0.000019 nm. They are in good agreement with the published values [18–20]. The C2N sample was monoclinic (space group $P2_1$) with refined parameters: a=0.768528±0.000012 nm, b=1.335868±0.000040 nm, c=0.549586±0.000010 nm, γ=98.2864±0.0098°, which give a satisfactory agreement when compared with the literature values [21]: a=0.7697(2) nm, b=1.3385(6), c=0.5502(1) nm, γ=98.34(6)°.

The measured data for CN involve 113 C_{pm} values from relaxation time, 28 points from DSC and 32 values of the enthalpy increments from the drop measurements. For C2N, 122 C_{pm} values from relaxation time, 28 points from DSC and 14 values of the enthalpy increments from the drop measurement were obtained. Low-temperature C_{pm} data are plotted in Figs 1 and 2, enthalpy increment data are listed in Tables 1 and 2.

The fit of the low-temperature heat capacity data consists of two steps. Assuming the validity of the phenomenological formula $C_{pm}=\beta T^3+\gamma_{el}T$, at $T\to 0$ where β is proportional to the Debye temperature and γ_{el} is the Sommerfeld coefficient, we plot the C_{pm}/T *vs.* T^2 dependence for $T<9$ K to estimate the γ_{el} value (see the insets in Figs 1 and 2). As expected, the electronic specific heat is negligible in both samples, CN and C2N, yielding the respective γ_{el} values $1.7\cdot 10^{-4}$ and $3\cdot 10^{-5}$ J mol^{-1} K^{-2}. Simultaneously, the C_{pm}/T *vs.* T^2 plot provides an estimation of the Debye temperature, as in this temperature range only the acoustic phonons are populated.

Table 1 Enthalpy increments of calcium niobate $CaNb_2O_6$

T/K	$H_m(T)–H_m(298.15)$/ kJ mol^{-1} Experimental	$H_m(T)–H_m(298.15)$/ kJ mol^{-1} Integration of Eq. (4)	δ/%$^{\#}$
669.4	75.3	74.1	–1.5
669.5	75.3	74.2	–1.5
723.4	86.5	85.9	–0.7
723.4	86.5	85.9	–0.7
769.4	96.9	96.0	–0.9
769.5	96.9	96.0	–0.9
773.7	99.6	96.9	–2.6
822.1	108.1	107.7	–0.4
822.4	108.2	107.8	–0.4
873.8	115.6	119.3	3.3
873.8	122.5	119.3	–2.6
922.2	130.2	130.3	0.1
922.2	130.1	130.3	0.1
974.0	137.3	142.2	3.6
974.0	135.4	142.2	5.0
1023.2	153.0	153.5	0.3
1023.2	153.1	153.5	0.3
1074.1	164.9	165.4	0.3
1122.6	175.6	176.8	0.7
1122.6	175.5	176.8	0.7
1173.9	191.3	189.0	–1.2
1173.9	190.2	189.0	–0.6
1222.6	198.4	200.7	1.1
1222.6	198.4	200.7	1.1
1273.8	220.6	213.0	–3.4
1273.8	211.0	213.0	1.0
1321.5	221.2	224.6	1.6
1321.6	221.0	224.6	1.6
1373.0	242.0	237.2	–2.0
1373.0	241.0	237.2	–1.6
1421.3	244.4	249.1	1.9
1421.5	244.4	249.1	2.0

$^{\#}$δ=100(calc. – exp.)/exp.

In the second step of the fit, both sets of the C_{pm} data (relaxation time+DSC) were considered. Analysis of the phonon heat capacity was performed as an additive combination of Debye and Einstein models. The phonon spectrum of a polyatomic compound contains three acoustic branches and $3n–3$ optical ones, where n is number of atoms per formula unit. In our case, i.e. 9 and 11 atoms/f.u., this represents 24 and 30 optical branches, respectively. This approach is indeed a simplification, since n should properly refer to the number of atoms per primitive unit cell containing, in both cases, four formula units. However, this would lead to an inadequate increase of parameters to be fitted. To reduce the number of adjustable parameters, several individual branches are grouped together

Table 2 Enthalpy increments of calcium niobate $Ca_2Nb_2O_7$

T/K	$H_m(T)–H_m(298.15)$/ kJ mol^{-1} Experimental	$H_m(T)–H_m(298.15)$/ kJ mol^{-1} Integration of Eq. (4)	δ/%$^{\#}$
774	125.9	122.4	–2.7
774	124.6	122.4	–1.7
874	147.1	150.5	2.3
874	151.1	150.6	–0.4
974	176.7	179.1	1.4
974	176.8	179.1	1.4
1074	204.9	208.1	1.6
1074	204.9	208.1	1.6
1174	233.3	237.6	1.8
1174	233.4	237.6	1.8
1274	262.1	267.4	2.0
1274	262.1	267.4	2.0
1373	297.0	297.4	0.1
1373	293.9	297.4	1.2

$^{\#}$δ=100(calc. – exp.)/exp.

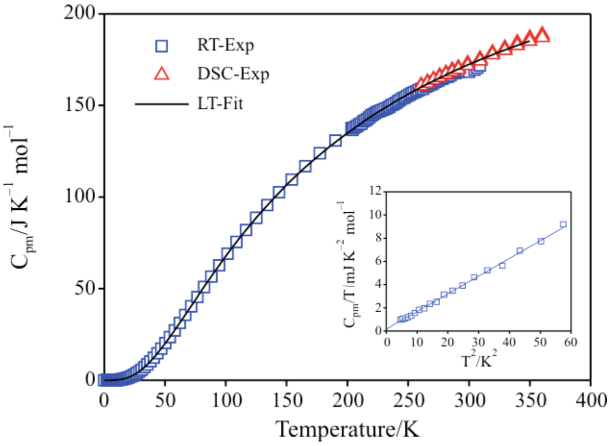

Fig. 1 Low-temperature heat capacity of $CaNb_2O_6$

Table 3 Parameters for the phonon heat capacity

Type	CN			C2N		
	Degeneracy	Θ_D or Θ_E/K	α_D or $\alpha_E/10^{-4}$ K^{-1}	Degeneracy	Θ_D or Θ_E/K	α_D or $\alpha_E/10^{-4}$ K^{-1}
Acoustic	3	234±1	3.0±0.1	3	218±1	0.5±0.1
Optical	1	148±1	2.5±0.1	4	177±1	0.5±0.1
	7	303±1	1.4±0.1	8	382±3	0.7±0.1
	8	502±1	0.8±0.1	8	448±6	0.7±0.1
	5	903±1	0.5±0.1	10	880±4	0.5±0.1
	3	1332±6	0.3±0.1			

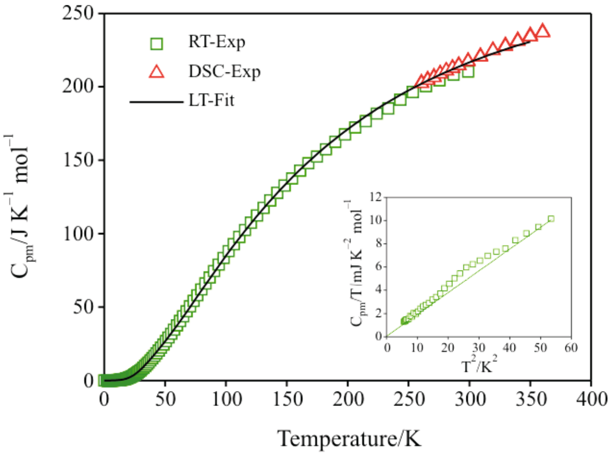

Fig. 2 Low-temperature heat capacity of $Ca_2Nb_2O_7$

into multiple degenerate branches with the same characteristic temperatures using a trial-and-error method.

Both models include corrections for anharmonicity, which is responsible for a small, but not negligible, additive term at higher temperatures and which accounts for the discrepancy between isobaric and isochoric heat capacity. According to literature [22], the term $1/(1-\alpha T)$ is considered as a correction factor.

The acoustic part of the phonon heat capacity is then described using the Debye model in the form

$$C_{\mathrm{phD}}=\frac{9R}{1-\alpha_{\mathrm{D}}T}\left(\frac{T}{\Theta_{\mathrm{D}}}\right)^3\int\limits_0^{x_{\mathrm{D}}}\frac{x^4\exp(x)}{(\exp(x)-1)^2}\mathrm{d}x \qquad (1)$$

where R is the gas constant, Θ_D is the Debye characteristic temperature, α_D is the coefficient of anharmonicity of acoustic branches and $x_D=\Theta_D/T$. Here the three acoustic branches are taken as one triply degenerate branch. Similarly, the individual optical branches are described by the Einstein model

$$C_{\mathrm{phEi}}=\frac{R}{1-\alpha_{\mathrm{Ei}}T}x_{\mathrm{Ei}}^2\frac{\exp x_{\mathrm{Ei}}}{(\exp x_{\mathrm{Ei}}-1)^2} \qquad (2)$$

where α_{Ei} and x_{Ei} have analogous meanings as in the previous case. Several optical branches are again grouped into one degenerate multiple branch with the same Einstein characteristic temperature and anharmonicity coefficient. The phonon heat capacity then reads

$$C_{\mathrm{ph}}=C_{\mathrm{phD}}+\sum_{i=1}^{3n-3}C_{\mathrm{phEi}} \qquad (3)$$

All the estimated values were included into the simplex routine [23] and a full non-linear fit was performed on all adjustable parameters. The analysis of the phonon heat capacity is summarized in Table 3.

The values $H_m(298.15)-H_m(0)=$ 28159±170 J mol^{-1} and $H_m(298.15)-H_m(0)=$ 35631±215 J mol^{-1} for CN and C2N, respectively, were obtained from the low-temperature C_{pm} data by numerical integration of the C_{pm} from zero to 298.15 K. Standard deviations (2σ) were calculated with the error propagation law.

The values of standard molar entropies of CN and C2N at 298.15 K S_m^0(CN, 298.15 K)= 167.3±0.9 J K^{-1} mol^{-1} and S_m^0(C2N, 298.15 K)= 212.4±1.2 J K^{-1} mol^{-1} were derived from the low-temperature C_{pm} data by integrating the C_{pm}/T functions from zero to 298.15 K. A numerical integration (trapezoidal rule) was used with the boundary conditions $S_m^0=0$ and $C_{pm}/T=\theta_{el}$ at $T=0$ K. Standard deviations (2σ) were calculated using the error propagation law. Our value S_m^0(CN, 298.15 K) is by 6.6% lower than the one quoted in tables [6]. As the calorimetric entropies are generally considered as more reliable than those derived from equilibrium measurements, we prefer the values obtained in this work.

For the assessment of C_{pm} function above room temperature, the heat capacity data from DSC and the enthalpy increment data from drop calorimetry were treated simultaneously. Different masses w_i were assigned to individual points calculated as $w_i=1/\delta_i^2$ where δ_i is the absolute deviation of the i^{th} measurement estimated from overall accuracies of the measurements (1% for DSC and 3% for drop calorimetry). Both types of experimental data thus gain comparable significance during the regression analysis. The temperature dependencies of the heat capacities of CN and C2N (T=298.15–1500 K) can thus be expressed by:

$$\text{CN: } C_{pm}=(200.4\pm4.0)+(0.03432\pm0.005431)T-\frac{(3.450\pm0.2245)\cdot10^6}{T^2}\ (\text{J K}^{-1}\ \text{mol}^{-1}) \qquad (4)$$

$$\text{C2N: } C_{pm}=(257.2\pm6.2)+(0.03621\pm0.001206)T-\frac{(4.435\pm0.2428)\cdot10^6}{T^2}\ (\text{J K}^{-1}\ \text{mol}^{-1}) \qquad (5)$$

The heat capacities as functions of temperature are shown in Figs 3 and 4. The pertinent functions calculated according to the additivity Neumann–Kopp's rule (NKR) [24] are given for comparison. C_p data for CaO and Nb_2O_5 were taken from Refs [25, 6], respectively. While NKR predicts the heat capacities of CN and C2N remarkably well from room temperature up to ~700 K, the differences between the two dependencies, $\Delta C_{p,ox}$, increase with increasing temperature. The prediction ability of NKR for mixed oxides was discussed in [26, 27], but it seems impossible now to state in which cases NKR will estimate the heat capacity with acceptable uncertainty in the high temperature region.

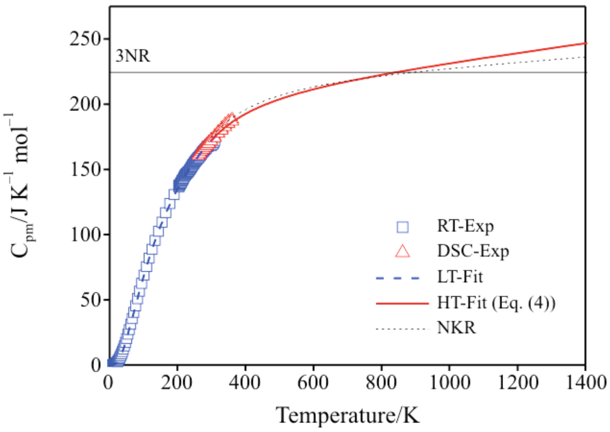

Fig. 3 Heat capacity of $CaNb_2O_6$

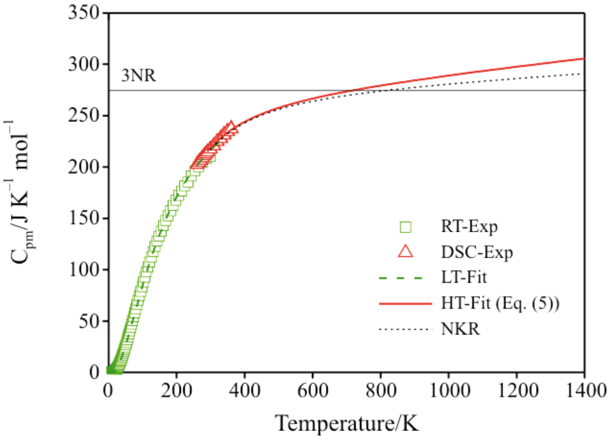

Fig. 4 Heat capacity of $Ca_2Nb_2O_7$

Based on the EMF measurements [7, 8] Raghavan has derived the Gibbs energy of formation of CN and C2N from the constituent binary oxides (CaO+Nb_2O_5): $\Delta_{f,ox}G^0(CaNb_2O_6$, 1274 K)= –118.44 kJ mol^{-1} and $\Delta_{f,ox}G^0(Ca_2Nb_2O_7$, 1256 K)= –178.44 kJ mol^{-1}. Given the relation

$$\Delta_{f,ox}G^0(T)=\Delta_{f,ox}H^0(T)-T\Delta_{f,ox}S^0(T) \qquad (6)$$

the $\Delta_{f,ox}S^0$ values can be calculated using the heat capacity and entropy data for CN a C2N obtained in this work and the literature values for CaO [25] and Nb_2O_5 [6]: $\Delta_{f,ox}S^0$(CN, 1274 K)= –8.2 J K^{-1} mol^{-1} and $\Delta_{f,ox}S^0$(C2N, 1256 K)=4.9 J K^{-1} mol^{-1}. Based on the third law, the $\Delta_{f,ox}H^0$ values are then calculated according to Eq. (6) and, using temperature dependences of C_{pm}, recast to 298.15 K: $\Delta_{f,ox}H^0(CaNb_2O_6$, 298.15 K)= –130.06 kJ mol^{-1} and $\Delta_{f,ox}H^0(Ca_2Nb_2O_7$, 298.15 K)= –177.54 kJ mol^{-1}. Finally, the standard enthalpies of formation of CN and C2N from elements were calculated from $\Delta_{f,ox}H^0$ adding appropriate sums of standard enthalpies of formation of CaO [25] and Nb_2O_5 [6]: $\Delta_fH^0(CaNb_2O_6$, 298.15 K)= –2664.52 kJ mol^{-1} and $\Delta_fH^0(Ca_2Nb_2O_7$, 298.15 K)= –3346.91 kJ mol^{-1}. The values of standard enthalpy of formation of CN at 298.15 K from the present evaluation and from tables [6] are almost the same.

Acknowledgements

This work was supported by the Czech Science Foundation (grant N° 104/07/1209) and Ministry of Education of the Czech Republic (research projects N° MSM6046137302 and N° MSM6046137307). The work of P.S. is a part of the research program MSM0021620834 financed by the Ministry of Education of the Czech Republic.

References

1 M. Ibrahim, N. F. H. Bright and J. F. Rowland, J. Am. Ceram. Soc., 45 (1962) 329.
2 A. Jongejan, J. Less-Common Met., 19 (1969) 193.
3 T. A. Vanderah, W. Febo, J. Y. Chan, R. S. Roth, J. M. Loezos, L. D. Rotter, R. G. Geyer and D. B. Minor, J. Solid State Chem., 155 (2000) 78.
4 V. G. Dneprova, T. N. Rezukhina and Ya. I. Gerasimov, Doklady Akad. Nauk SSSR, 178 (1968) 135.
5 O. Kubaschewski, High Temp. – High Pressures, 4 (1972) 1.
6 O. Knacke, O. Kubaschewski and K. Hesselmann (Eds.), Thermochemical Properties of Inorganic Substances, 2nd Ed., Springer, Berlin 1991, p. 384.
7 S. Raghavan, Trans. Indian Inst. Met., 44 (1991) 285.
8 S. Raghavan, J. Alloys Compd., 179 (1992) L25.

9 P. Abrman, D. Sedmidubský, A. Strejc, P. Voňka and J. Leitner, Thermochim. Acta, 381 (2002) 1.

10 M. Hampl, A. Strejc, D. Sedmidubský, K. Růžička, J. Hejtmánek and J. Leitner, J. Solid State Chem., 179 (2006) 77.

11 M. Hampl, J. Leitner, K. Růžička, M. Straka and P. Svoboda, J. Therm. Anal. Cal., 87 (2007) 553.

12 J. Leitner, M. Hampl, K. Růžička, D. Sedmidubský, P. Svoboda and J. Vejpravová, Thermochim. Acta, 450 (2006) 105.

13 J. Leitner, M. Hampl, K. Růžička, M. Straka, D. Sedmidubský and P. Svoboda, J. Therm. Anal. Cal., 91 (2008) 985.

14 J. S. Hwang, K. J. Lin and C. Tien, Rev. Sci. Instrum., 68 (1997) 94.

15 W. Schnelle, J. Engelhardt and E. Gmelin, Cryogenics, 39 (1999) 271.

16 Quantum Design, Physical Property Measurement System – Application Note, http://www.qdusa.com/pdf/brochures/heat.pdf.

17 J. W. Arblaster, Platinum Metals Rev., 38 (1994) 119.

18 J. P. Cummings and S. H. Simonsen, Am. Miner., 55 (1970) 90.

18 R. M. Rakhmankulov and Yu. P. Udalov, Zh. Neorg. Khim., 21 (1976) 2842.

20 V. I. Spitsyn, E. A. Ippolitova, L. M. Kovba, L. N. Lykova and P. P. Leshchenko, Zh. Neorg. Khim., 27 (1982) 827.

21 N. Ishizawa, F. Marumo, S. Iwai, M. Kimura and T. Kawamura, Acta Cryst., B36 (1980) 763.

22 C. A. Martín, J. Phys. Condens. Matter, 3 (1991) 5967.

23 W. H. Press, S. A. Teukolsky, W. T. Vetterling and B. P. Flannery, Numerical Recipes in FORTRAN, 2nd Ed., Ch. 10.4, pp. 402–406, Cambridge University Press, 1992.

24 J. Leitner, P. Chuchvalec, D. Sedmidubský, A. Strejc and P. Abrman, Thermochim. Acta, 395 (2003) 27.

25 J. R. Taylor and A. T. Dinsdale, CALPHAD, 14 (1990) 71.

26 P. Richet and G. Fiquet, J. Geophys. Res., 96 (1991) 445.

27 L. Qiu and M. A. White, J. Chem. Educ., 78 (2001) 1076.

DOI: 10.1007/s10973-008-9245-2